6.1 Introduction

In chapter 1, it was already discussed that the pyrometallurgical route dominates the metal production due to the energy efficient and cheaper. Pyrometallurgical route of metal extraction from stable oxides like silica, alumina by the carbothermic reduction needs very high temperature which creates many problems for metal yield (Halmann et al., 2007).

Conventionally the production of metallurgical grade silicon is happened by the reduction of silicon dioxide with carbon in an electric arc furnace (Fairchild, 1970). Various researchers were proved the formation of SiO in the carbothermic reduction of silica during the silicon production as SiO_2 (s) + C (s) = SiO (g) + CO (g) (Eriksson and Johansson, 1978; Hutchison et al., 1988; Johansson and Eriksson, 1980; Krivsky and Schuhmann, 1961). Slag-metal partitioning reaction during silicon production is mainly responsible for the silicon yield (Turkdogan et al., 1980).

Many attempts were taken for direct production of aluminium from their oxides, but route could not be established. Metallic aluminium is produced only above 1980°C by carbothermic reduction of their oxides. Due to its high vapor pressure at that temperature, aluminium gets vaporize. The overall reactions in the carbothermic reduction of alumina could be driven in the forward direction only either decreasing the activity of the aluminium or reducing the partial pressure of CO.

$Al_2O_3 + 3C \leftrightarrow 2Al + 3CO$;…….(6.1)

The second option is ruled out as it increases the volatilization losses of the metal at that operating temperature. The activity of aluminium could be decreased by dissolving it in some liquid metal solvent to form an alloy and compound (Howell et al., 1988). It could be achieved by reducing alumina with some metal oxide.

$Al_2O_3 + 2MO + 4C = 2(Al\text{-}M) + 4CO$;…….(6.2)

The substantial lowering of the activity to achieve these advantages but could not separate out from the solvent so easily. However, to overcome these limitation and to take the benefits of liquid metal as a solvent, which should interact selectively to metallic phase to suppress the activity of aluminium in the bath without stabilizing the carbide, oxy-carbide or oxide phases. Thermodynamically the selection criteria for solvent metal should be such that it forms a nearly ideal solution with aluminium (Elliott and J.F., 1989). Solvent metals that cause large negative deviation will tend to form intermetallic. This compound creates difficulty in separation by simple means as a fractional crystallization. The solvent metals should not have a high vapor pressure at the operating temperature to minimize the volatilization loss. The metals that satisfy most of the above conditions are silver, gold, platinum tin or copper. Because of economic consideration, silver, gold, platinum could not be used commercially as solvent metals.

Besides these, silicon which is thermodynamically not so favorable solvent metal, but also could be formed during the smelting of waste materials, the major oxides present in waste are silica followed by alumina (Mandal and Sinha, 2014). Therefore, the probability of producing aluminium silicon alloy will be more as

$Al_2O_3 + 2SiO_2 + 7C = 2(Al\text{-}Si) + 7CO$;……(6.3).

Iron oxide is also present in the waste material, therefore the product may also form (Al-Si-Fe) as

$Al_2O_3 + 2SiO_2 + Fe_2O_3 + 10C = 2(Al\text{-}Si\text{-}Fe) + 10CO$;…….(6.4).

The increased content of the iron oxide in the waste may be helpful for the absorption of aluminium and silicon both. At the temperature for reduction of alumina/silica, the reduced iron converts into the liquid state. Therefore, the absorption of reduced aluminium, silicon in

the molten iron will be useful. From this alloy containing aluminium with other metals could be extracted using a variety of separation techniques such as electrolytic, crystallization, distillation etc.

From 1920, arc furnace route was used to make aluminium silicon alloy, which was modified by Alcan process to make Al-Si-Fe alloy (Johansen et al., 2003). In 1977, Alcoa process was established for the production of Al-Si-Fe alloy by blast furnace route (Bruno, 1982) . In 1973, Kawara developed a blast furnace process with extra heat from electricity to produce Al-Si-Fe alloy (Kuwahara, 1983). It was subjected to purification by dissolving aluminium in molten lead at 1200-1300°C to form Al-Pb alloy (Mankhand, 2011).

Wang et al. (2010) were patented technology to reduce bauxite flotation tailings in an electric arc furnace to produce a high aluminum alloy at 2573–2773K (2300-2500°C). They were also reported the formation of an Al–Si alloy at above 2073K (1800°C) temperature. They were claimed for the optimum conditions of Al–Si alloy production is pressure at 0.1 MPa, temperature of 2173K (1900°C), the carbon content of 95% of the theoretical amount, and one hour heating time.

Pickles et al, 1990 were recovered the metal values from fly ash by argon plasma in an extended arc flash reactor (EAFR). That process successfully recovered silicon and iron. At that high temperature, produced aluminum got vaporized out through exit gas.

From the literature, it was evidenced that, extraction of metals from the waste material containing silica, alumina as a major constituent, could be possible through high-temperature carbothermic reduction.

The present investigation is to aim for recovering aluminum along with other metals such as iron, silicon, manganese etc. through the smelting reduction of iron ore slime and

bottom ash under different arc exposure conditions of indigenously fabricated transferred arc plasma (TAP) furnace.

6.2. Experimental

6.2.1. Raw Materials

The PCC bottom ash was used in this study along with iron ore slime for the recovery of multi-metallic components. The mild steel scrap was used for the generation of liquid steel bath as a solvent for the absorption of reduced metals. The analysis of raw materials used for this present study is mentioned in Table 6.1.

Table 6. 1 Analysis of raw materials

Bottom ash		**Reductants (dry basis)**				**Iron ore slime**		**Mild steel scrap**	
Composition	Wt.%	Proximate analysis	Char (wt.%)	Coal (wt.%)	Graphite (wt.%)	Composition	wt.%	Composition	wt.%
SiO_2	70.04	V.M	33.72	18.6	0.40	SiO_2	31.36	C	0.04
Al_2O_3	22.05	Ash	5.80	11.2	4.10	Al_2O_3	24.11	Si	0.10
Fe_2O_3	2.49	F.C	60.48	70.2	95.5	Fe_2O_3	42.09	Mn	0.80
MgO	1.18					CaO	0.02	S	0.03
CaO	0.76					P_2O_5	1.48	P	0.04

Wood char, coal and graphite powder of 0.5 mm size were used to mix with bottom ash or bottom ash + iron ore slime for making pellets, using as a charging material. Granules of respective reductants (-2 mm size) were mixed with bottom ash or bottom ash + iron ore slime powder as another form of charge material. A different form of charge materials and their respective mix proportion are shown in Table 6.2. For making pellet samples, a disk pelletizer having diameter 760 mm, rim height 120 mm, disc angle 45°, r.p.m. 20 was used. The addition of 5% bentonite was done for increasing pelletizing efficiency and providing green strength in the pellets. Green pellets were dried at 383K (110°C) for 4 hours to remove moisture as well

as achieve adequate strength for further processing. The photographs of different raw materials used in this present study are shown in Figure 6.1.

Table 6. 2 Mix proportion of feed materials

Charge material code	Charge material type	Charge material composition				Reductant type	Reductant carbon content
		Bottom ash	Iron ore slime	Bentonite	Reductant		
P1	Pellet	70 %	0 %	05 %	25 %	Char	Stoichiometry
P2	Pellet	35 %	35 %	05 %	25 %	Char	Stoichiometry
P3	Powder	250 g	0 g	0 g	150 g	Coal	Stoichiometry
P4	Powder	125 g	125 g	0 g	150 g	Coal	Stoichiometry
P5	Powder	310 g	0 g	0 g	90 g	Graphite	Stoichiometry
P6	Powder	155 g	155 g	0 g	90 g	Graphite	Stoichiometry
P7	Powder	230 g	0 g	0 g	170 g	Char	Stoichiometry
P8	Powder	115 g	115g	0 g	170 g	Char	Stoichiometry
P9	Powder	115 g	0 g	0 g	85 g	Char	Stoichiometry
P10	Powder	57.5g	57.5g	0 g	85 g	Char	Stoichiometry
P11	Powder	160 g	0 g	0 g	240 g	Char	Double
P12	Powder	80 g	80g	0 g	240 g	Char	Double
P13	Powder	290 g	0 g	0 g	110 g	Char	Half
P14	Powder	145 g	145 g	0 g	110 g	Char	Half
P15	Powder	400 g	0 g	0 g	0 g	0 g	-
P16	Powder	200 g	200 g	0 g	0 g	0 g	-

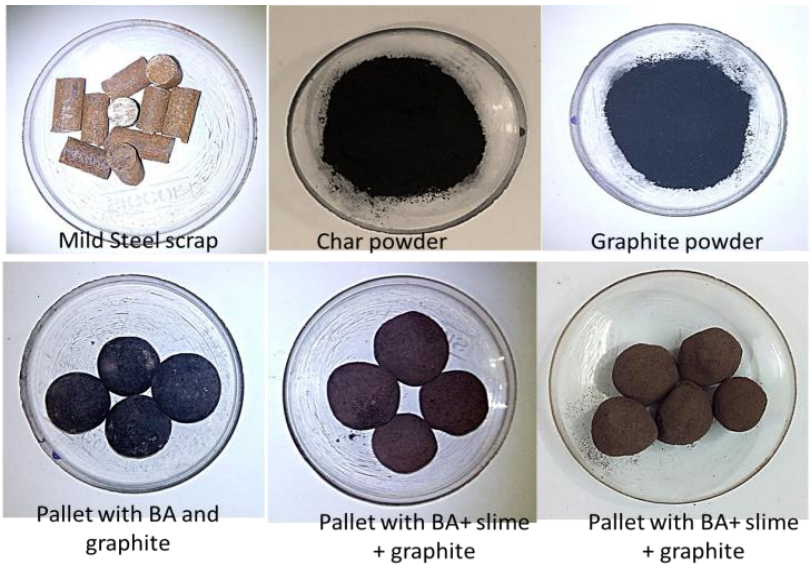

Figure 6. 1 Photographs of raw material used in the present study

6.2.2 Smelting Furnace

Indigenously fabricated transfer arc plasma (TAP) furnace was used in the present study. Both types of crucible material such as graphite and magnesite were used separately for smelting reduction studies. The operational characteristics of this furnace for its suitability were already described in the previous chapter-5 under design and fabrication section. The nitrogen gas for generating plasma was passed through a hollow graphite electrode to reach near the arc zone for generating a large number of nitrogen ions/ atoms resulting high temperatures (Sinha and Gupta, 1993). The flow rate of nitrogen gas was fixed to 6.67×10^{-5} m^3/s during charging of pellets.

6.2.3 Smelting procedure

To melt 1 kg steel scrap, initially around 500 grams of steel scrap was charged in the crucible before switching on the power. The melting was initiated by striking the arc with using solid or hollow electrode respectively. When the initial charge got melted completely, then gradually remaining scraps were charged continuously through the charging hole above the roof. After complete melting of the charge, first heat was tapped out as a ‘flush-heat’ or ‘washed heat’ to avoid excess carbon pick up from the crucible (in the case of graphite crucible) and mean time the furnace become super-heated.

After wash heat, a new heat was made immediately as the procedure described in Figure 6.2. A hollow one electrode then replaced solid electrode after preparing a complete liquid bath. Plasma gas was introduced through hollow electrode followed by addition of charge material (pellet/ powder mixture) at the plasma zone gradually. The charging was done through a hopper fixing on the charging door above the roof of the furnace. After complete dissolution of charge material, samples were taken out at different interval of time for composition

analysis. For comparison of different plasma (N_2/H_2), one heat each was started melting under such plasma condition respectively.

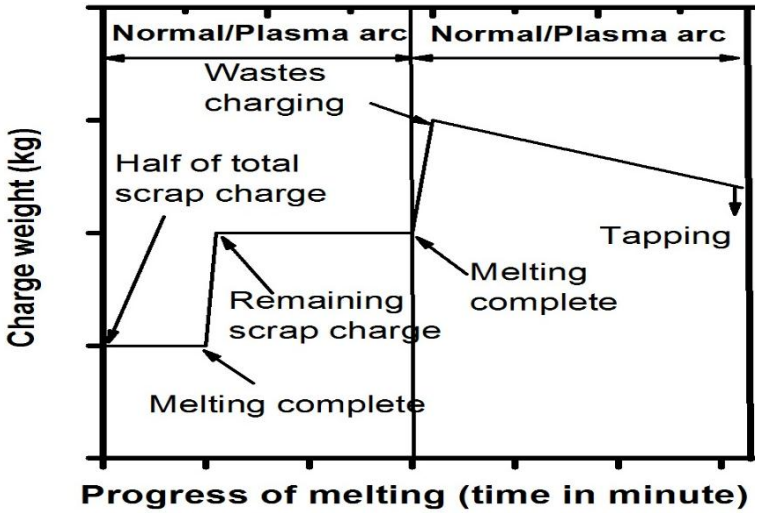

Figure 6. 2 Melting procedure flow chart

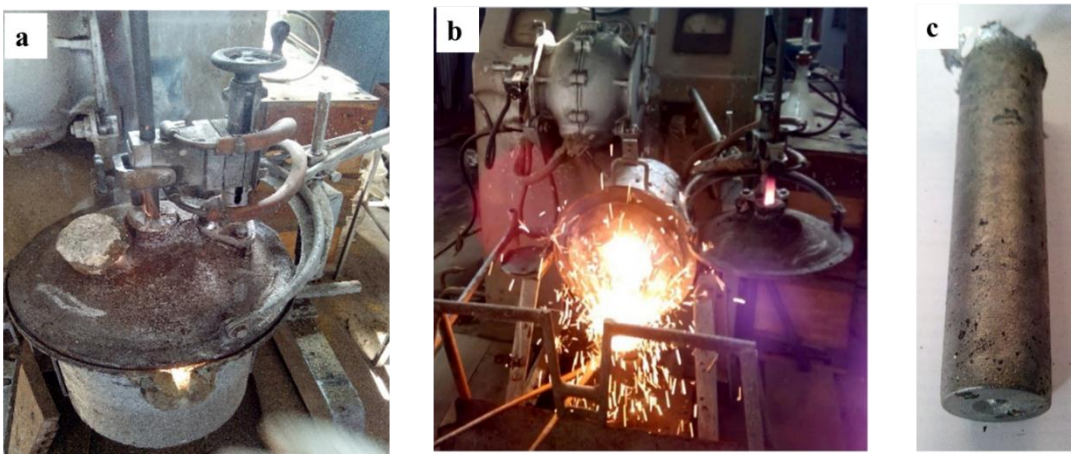

Figure 6. 3 Photographs of a) Melting operation b) Pouring operation c) Cast ingot

Figure 6.3 shows the photograph of the furnace during melting process and tapping of liquid metal in the round graphite mould of 35 mm diameter as well the produced solid ingot of 35 mm diameter. The round sample from the different ingots was cut like a slice of 10-15 mm thick for chemical analysis through optical emission spectroscopy (OES).

Table 6. 3 Charge composition used for different melting

Melting Code	Heat No	Charge material	Crucible material	Ionizing Gas	Exposure time (min)	Reductant type	Charge Material	Carbon Content	Pellet Chemistry
			(G-Graphite M-Magnesite)	(N-Nitrogen H-Hydrogen A-Normal arc)		(Ch-Char Co-Coal Gr-Graphite)	(Pe-Pellet Po-Powder)	(S- stoichiometry 2S- Double stoichiometry 1/2S- Half stoichiometry)	(B-Bottom ash B+S-Bottom ash and iron ore slime)
P1C1G1T1	1	1	G	N	10	Ch	Pe	S	B
P1C1G1T2	1	1	G	N	20	Ch	Pe	S	B
P1C1G1T3	1	1	G	N	30	Ch	Pe	S	B
P1C1G1T5	1	1	G	N	50	Ch	Pe	S	B
P1C1G1T8	1	1	G	N	80	Ch	Pe	S	B
P2C1G1T1	2	2	G	N	10	Ch	Pe	S	B+S
P2C1G1T2	2	2	G	N	20	Ch	Pe	S	B+S
P2C1G1T3	2	2	G	N	30	Ch	Pe	S	B+S
P2C1G1T5	2	2	G	N	50	Ch	Pe	S	B+S
P2C1G1T8	2	2	G	N	80	Ch	Pe	S	B+S
P7C2G1T3	3	7	M	N	30	Ch	Po	S	B
P8C2G1T3	4	8	M	N	30	Ch	Po	S	B+S
P9C2G1T3	5	9	M	N	30	Ch	Po	S	B
P10C2G1T3	6	10	M	N	30	Ch	Po	S	B+S
P7C1G1T3	7	7	G	N	30	Ch	Po	S	B
P8C1G1T3	8	8	G	N	30	Ch	Po	S	B+S
P3C2G1T3	9	3	M	N	30	Co	Po	S	B
P4C2G1T3	10	4	M	N	30	Co	Po	S	B+S
P5C2G1T3	11	5	M	N	30	Gr	Po	S	B
P6C2G1T3	12	6	M	N	30	Gr	Po	S	B+S
P13C2G1T3	13	13	M	N	30	Ch	Po	1/2S	B
P14C2G1T3	14	14	M	N	30	Ch	Po	1/2S	B+S
P11C2G1T3	15	11	M	N	30	Ch	Po	2S	B
P12C2G1T3	16	12	M	N	30	Ch	Po	2S	B
P15C2G2T3	17	15	M	H	30	0	Po	0	B
P16C2G2T3	18	16	M	H	30	0	Po	0	B+S
P7C2G2T3	19	7	M	H	30	Ch	Po	S	B
P8C2G2T3	20	8	M	H	30	Ch	Po	S	B+S
P7C2G0T3	21	7	M	A	30	Ch	Po	S	B
P8C2G0T3	22	8	M	A	30	Ch	Po	S	B+S

Slag was skimmed out before pouring/tapping. XRF analysis has also performed the metal and analysis of slag.

Table 6.3 shows the different charge composition which was used during melting operation to observe the recovery of various elements on following operating parameters:

i) effect of mixture ratio of bottom ash and iron ore slime, ii) charge in the form of pellet and powder, iii) different reactivity of reductant such as char, coal, graphite, iv) stoichiometric ratio of carbon content, v) charge layer thickness, vi) crucible lining materials, vii) arc type, and viii) melting time.

6.3 Results and Discussions

Chemical analysis of the products (ingots) after smelting reduction studies using different types of charge material was performed, and results are shown in Table 6.4.

6.3.1 Recovery of major elements in metals

Based on the analysis shown in Table 6.4, the recovery of major elements in metals was calculated on following parameters. The calculated recovery values of different main elements are shown in Table B.7 of Appendix-B. The effect of various operating parameters on the recovery of different elements are discussed under following sections.

6.3.1.1 Melting time

Analysis of different samples taken out at a various interval of time (10, 20, 30, 50,80 minutes) of heat number 1 and 2 are being illustrated in the Figure 6.4 a and 6.4 b for charge of bottom ash as well as mixture of bottom ash and iron ore slime respectively.

Table 6. 4 Chemical composition of major elements present inside the ingots

Melting Code	Heat No	Chemical composition (wt%)			
		Fe	Si	Al	Mn
P1C1G1T1	1	92.31	4.90	0.47	0.37
P1C1G1T2	1	94.00	2.70	0.82	0.51
P1C1G1T3	1	93.40	3.15	1.02	0.57
P1C1G1T5	1	93.40	3.78	0.90	0.53
P1C1G1T8	1	92.00	6.90	0.56	0.49
P2C1G1T1	2	94.50	1.65	0.75	0.45
P2C1G1T2	2	93.80	2.35	1.08	0.52
P2C1G1T3	2	93.50	2.76	1.25	0.56
P2C1G1T5	2	93.00	3.80	1.22	0.54
P2C1G1T8	2	92.70	5.51	1.02	0.49
P7C2G1T3	3	92.91	3.33	1.36	0.43
P8C2G1T3	4	91.56	2.61	0.81	0.48
P9C2G1T3	5	93.39	1.05	0.32	0.56
P10C2G1T3	6	92.93	3.70	1.20	0.49
P7C1G1T3	7	93.27	3.17	1.52	0.37
P8C1G1T3	8	92.55	3.50	1.52	0.43
P3C2G1T3	9	93.73	3.05	0.95	0.41
P4C2G1T3	10	92.05	4.25	1.43	0.39
P5C2G1T3	11	95.53	1.61	0.56	0.49
P6C2G1T3	12	95.18	1.70	0.83	0.34
P13C2G1T3	13	95.21	2.20	0.72	0.45
P14C2G1T3	14	94.13	2.40	1.01	0.30
P11C2G1T3	15	93.21	2.70	1.05	0.46
P12C2G1T3	16	91.57	2.75	1.00	0.31
P15C2G2T3	17	92.15	2.02	1.05	0.44
P16C2G2T3	18	97.06	1.99	0.43	0.31
P7C2G2T3	19	91.48	5.07	0.71	0.57
P8C2G2T3	20	93.60	3.70	0.60	0.46
P7C2G0T3	21	94.74	2.35	1.04	0.38
P8C2G0T3	22	95.39	1.60	0.63	0.40

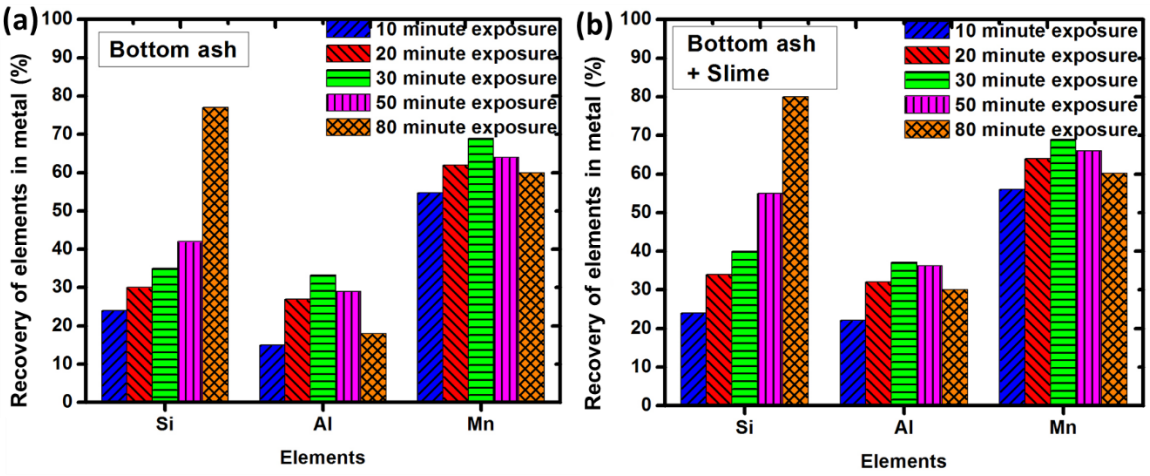

Figure 6. 4 Effect of exposure time on recovery of elements in metal

It was seen from the figure that with increasing nitrogen plasma exposure time, the recovery of elements was increased in metal. It may be due to the reduction of fused oxides increases with increasing exposure time in presence of the carbon. In the meantime, the reduced metals were absorbed by the steel bath. The maximum recovery of metals was observed upto 30 minutes of exposure time. After exposure for 30 minutes time, the metals recovery were observed decreasing trends in all the cases. Excess exposure time may be vaporized or reoxidized to some extent resulting the reduction in recovery level.

In the case of silicon, by increasing exposure time beyond 50 minutes, a drastic increase in the recovery level was observed. It may be occurred due to the erosion of crucible lining for both types of charge material. Recovery level was found slightly more for charge containing a mixture of bottom ash and iron ore slime as compared to only bottom ash.

6.3.1.2 Reactivity of reductant

Recovery of elements in metal for heat number 3, 9, 11 as well as 4, 10, 12 at varying reactivity of reductants is shown in Figure 6.5a and 6.5b for the charge of bottom ash as well as a mixture of bottom ash and iron ore slime respectively. Three different types of reductant having very

high reactivity (i.e. char), medium reactivity (i.e. coal) as well as lower reactivity (i.e. graphite) were used to study the effect of reductant reactivity on the recovery of different metals. For the same plasma exposure time (i.e. 30 minutes), the recovery of various metals was observed as decreasing trends with decreasing reactivity of reductant for both types of charge materials. It may be due to the high reactivity of the reductant reduces the oxides of bottom ash & iron ore slime efficiently and the liquid melt absorbed reduced metals. Increased recovery level of metals was observed in all cases for charge containing a mixture of iron ore slime and bottom ash as compared to only bottom ash.

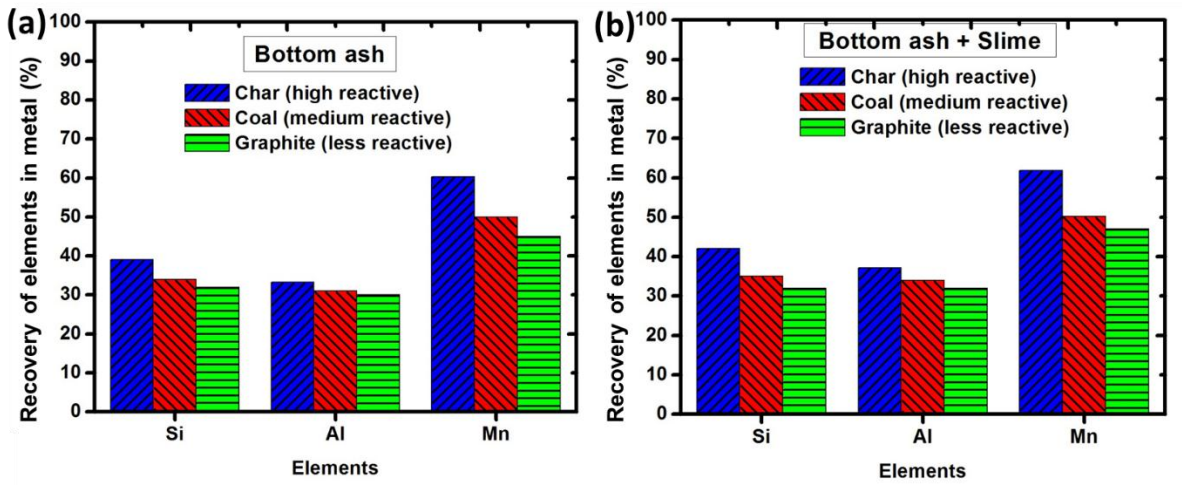

Figure 6. 5 Effect of reductant reactivity on recovery of elements in metal

6.3.1.3 Types of arc

The recovery of elements in metal for heat number 21, 03, 19 as well as 22, 04, 20 at different arcing condition (i.e. normal arc, nitrogen plasma, hydrogen plasma) are shown in Figure 6.6a and 6.6b for bottom ash as well as a mixture of bottom ash and iron ore slime charge material respectively. The absorption rate of elements in metals for all the cases was observed increasing trends in nitrogen plasma as compared to the normal arc. But in the case of hydrogen plasma, except aluminium, the recovery level of all elements were increased. At high

temperature and reducing atmosphere, the volatile aluminum went out with off gas without absorbing in metal bath, resulting less recovery of aluminium was noticed. The overall increment of absorption level was observed more in the case of charge containing a mixture of bottom ash and iron ore slime as compared to only bottom ash.

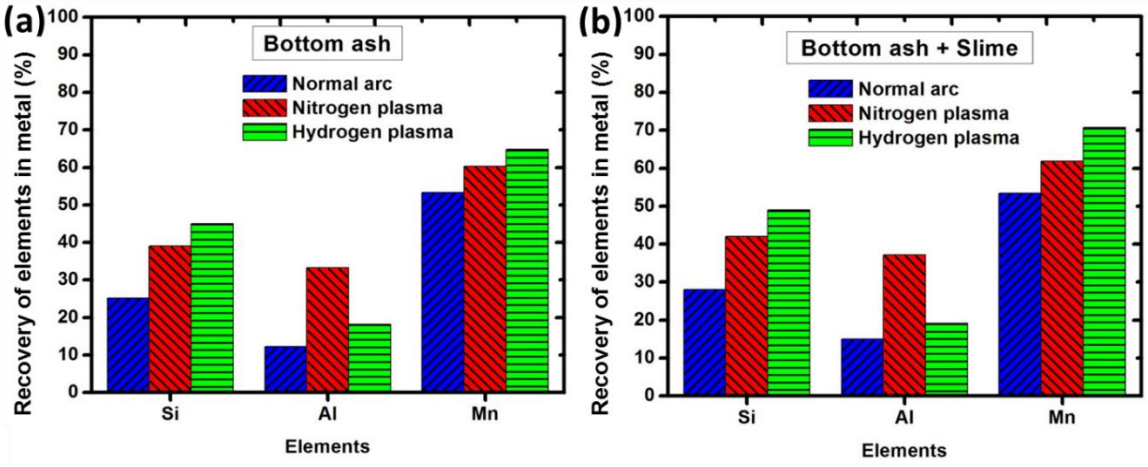

Figure 6. 6 Effect of arc on recovery of elements in metal

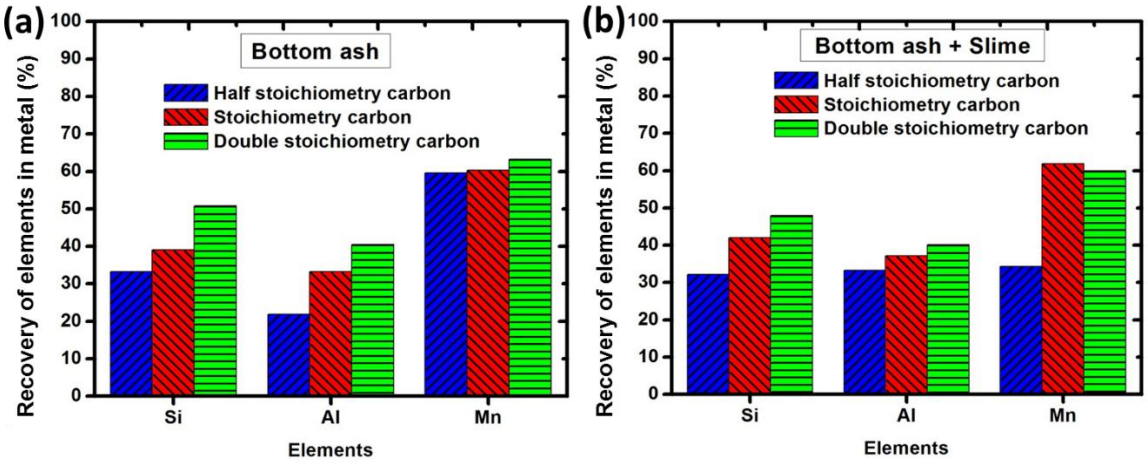

Figure 6. 7 Effect of stoichiometry of carbon content on recovery of elements in metal

6.3.1.4 Stoichiometric ratio of carbon content

Recovery of elements in metal for heat number 13, 03, 15 as well as 14, 04, 16 at different stoichiometry ratio of carbon (i.e. half, normal and double) are shown in Figure 6.7a and 6.7b

for bottom ash as well as a mixture of bottom ash and iron ore slime respectively. The recovery of elements in the metal bath was increased with increasing carbon content in the charge. Therefore, increasing carbon content (i.e. increasing stoichiometry), more reduction may be possible, resulting in more recovery. But increasing carbon content beyond the stoichiometry, the effect did not observe too much. The recovery level was found more for charge containing a mixture of iron ore slime and bottom ash as compared to only bottom ash.

6.3.1.5 Charge form

Recovery of elements in metal for heat number 01, 07 as well as 02, 08 at a different form of charge (i.e. pellets, powder) are shown in Figure 6.8a and 6.8b for bottom ash as well as a mixture of bottom ash and iron ore slime respectively. The lower recovery level of elements was observed in the case of pellets charge as compared to powder for bottom ash as well as a mixture of bottom ash and slime. It may be due to the effective covering of arc zone by powder as compared to pellet. It was effected as submerged like arcing, resulting in lower heat loss. The powder charge was also restricted the easy escaping of volatile metals (like aluminium) vapor as well as their suboxides.

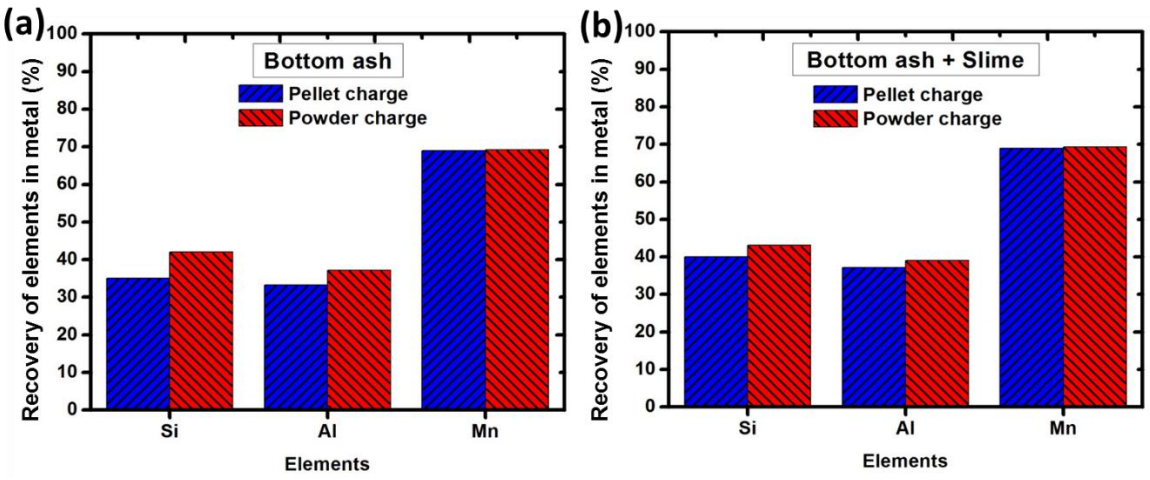

Figure 6. 8 Effect of form of charges on recovery of elements in metal

It may be absorbed by viscous slag followed by the dissolution reaction at the slag-metal interface. Therefore in this condition, the absorption efficiency may be increased.

6.3.1.6 Charge layer thickness

The recovery of elements in metal for heat number 05, 03 as well as 06, 04 at different charge layer thickness (i.e. half, normal) are shown in Figure 6.9a and 6.9b for bottom ash as well as a mixture of bottom ash and iron ore slime respectively. The recovery of elements in the metal bath was increased by increasing the charge quantity (it means increased charge layer thickness). The increasing charge layer thickness was reduced the heat loss. It was also increased for the entrapment of volatile metal vapor in the layer which was gradually moved downward for further absorption by steel bath as discuss above section 6.3.1.5. These two combined effects were increased the overall absorption rate of the elements by the metal bath.

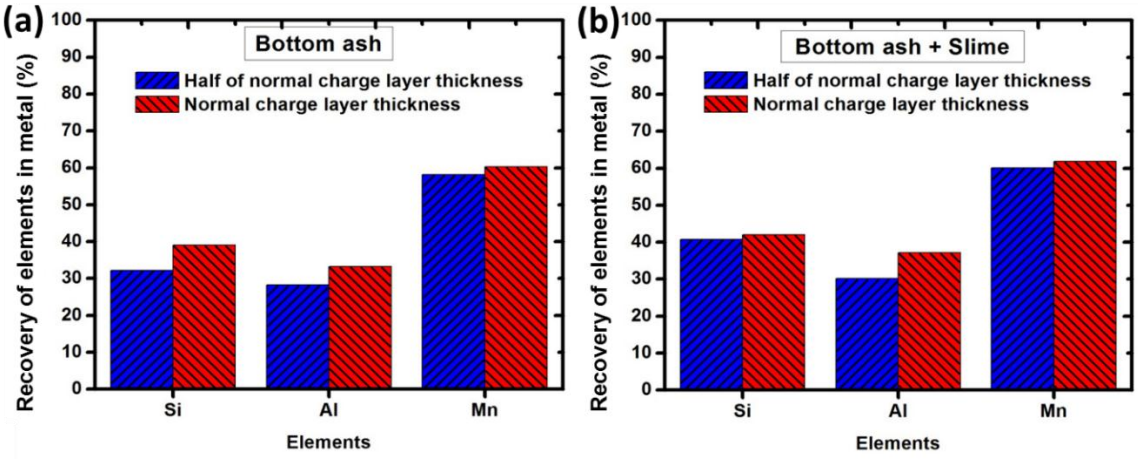

Figure 6. 9 Effect of charge layer thickness on recovery of elements in metal

6.3.1.7 Crucible lining materials

The recovery of elements in metal for heat number 03, 07 as well as 04, 08 at different types of crucible lining (i.e. magnesite and graphite) are shown in Figure 6.10a and 6.10b for bottom ash as well as a mixture of bottom ash and iron ore slime respectively. The recovery of elements

was increased in the case of graphite crucible as compared to magnesite crucible. The absorption of carbon by the liquid steel bath from the graphite crucible has happened. The carbon saturated metal bath was taken part in the reduction reaction with fused oxide charge layer at the slag-metal interface, resulting increasing the recovery level.

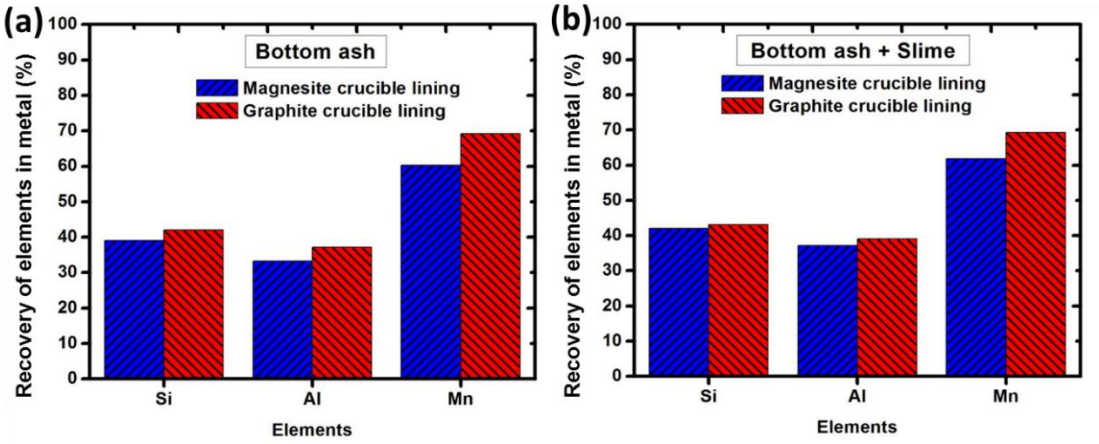

Figure 6. 10 Effect of crucible lining material on recovery of elements in metal

6.3.1.8 Effect of reducing agents

The recovery of elements in metal for heat number 17, 03, 19 as well as 18, 04, 20 at different reducing agent (i.e. hydrogen, nitrogen+carbon, hydrogen+carbon) are shown in Figure 6.11a and 6.11b for bottom ash as well as a mixture of bottom ash and iron ore slime respectively.

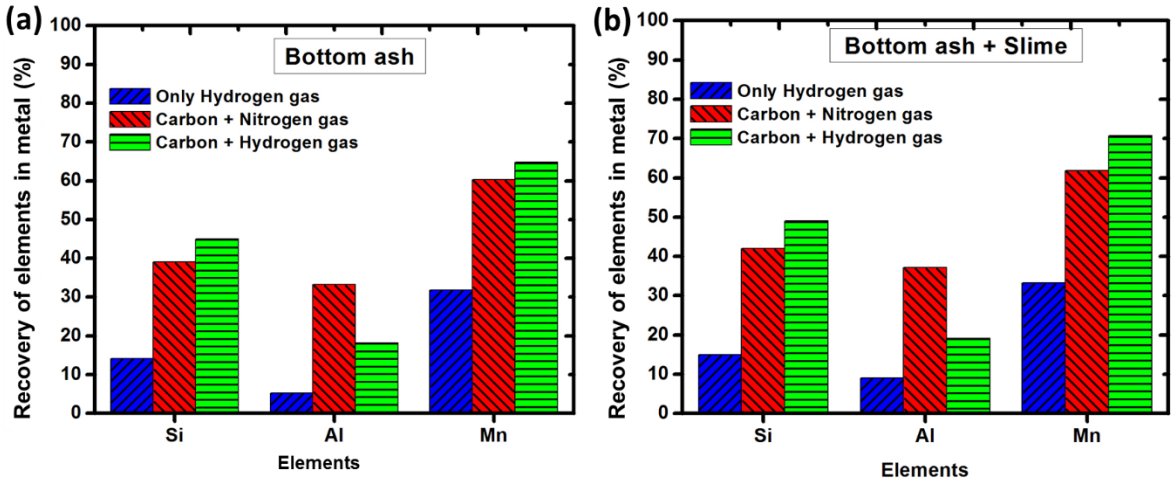

Figure 6. 11 Effect of reducing gas on recovery of elements in metal

From the figure, it is evident that the reducing gas (i.e. hydrogen) did not take part much in the reduction of oxides in the absence of carbon. A good recovery of elements in metals was observed in the case of a mixture containing carbon under nitrogen plasma exposure. Recovery of elements in the presence of carbon under inert nitrogen plasma environment, was good especially the metals of highly stable oxides like silica and alumina. It also indicated that the carbothermic reduction is essential for reduction of highly stable oxides like alumina and silica. At high temperature, hydrogen plasma could react either with produced metal or carbon due to its reducing nature. The reduction potentiality of reductant may decrease by consuming the carbon with reacting hydrogen gas. The hydrogen may also react with produced metal/metal suboxide. This combined effect resulted in not so pronounced recovery of elements in metal in spite of the combined effect of reducing agents (i.e. hydrogen and carbon).

6.3.2 Tentative mechanism of smelting

Figure 6.12 shows the Ellingham's diagram of the major oxides present in the waste materials used in present smelting study. It shows the order of carbothermic reaction on temperature as: Fe <Mn <Si <Mg <Al. On the other hand, the order of boiling points of these metals is Mg <Mn <Al <Si <Fe. This indicates that the reduction of alumina occurs at a higher temperature where aluminium metal exists in the form of vapor. Thermodynamically feasible reactions of carbothermic reduction for present case are as follows:

$3Fe_2O_3 + C = 2Fe_3O_4 + CO$ (g)……....(6.5)

$Fe_3O_4 + C = 3FeO + CO$ (g)……..…..(6.6)

$FeO + C = Fe + CO$ (g)…….…….…..(6.7)

$MnO + C = Mn + CO$ (g)…….……...(6.8)

$SiO_2 + C = SiO$ (g) + CO (g)…….…..(6.9)

$SiO\ (g) + C = Si + CO\ (g)$……..…....(6.10)

$Al_2O_3 + 2C = Al_2O\ (g) + 2CO\ (g)$….…….(6.11)

$Al_2O\ (g) + C = 2Al + CO(g)$……..…(6.12)

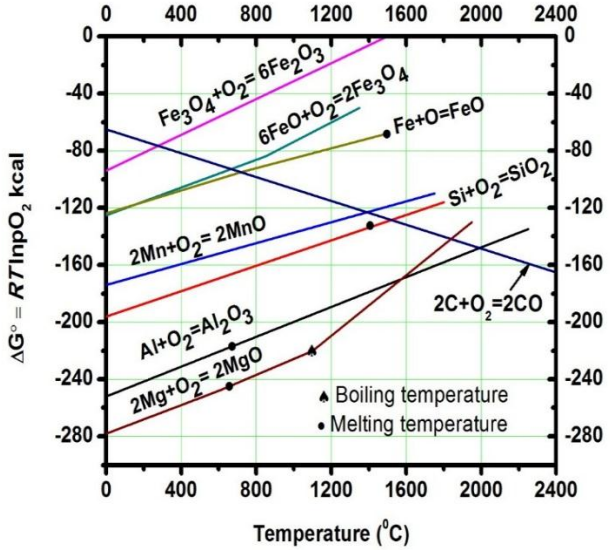

Figure 6. 12 Ellingham's diagram of major oxides present in the charge materials

During the reduction of iron oxide to iron, intermediate products of lower oxides (i.e. Fe_3O_4, FeO) do not exist in gaseous product form. But in the case of silica and alumina, they could produce intermediate products as silicon monoxide and aluminium monoxide in gaseous phase, respectively. Due to the lower vaporization temperature of aluminium, produced aluminium after reduction is converted into vapor at reduction temperature if not alloyed by iron metal pool immediately. Then it may escape out from the furnace along with the off gases.

Figure 6.13 illustrates the tentative mechanism for metals absorption by liquid iron bath on varying operating conditions. When the feeding of the charge materials occurred near the arc zone either in the form of pellets or power, it gradually fused and melted due to intense heat from the plasma arc. This melted oxide layer is often called slag layer mixture of silica, alumina, and other oxides along with reducing agent (carbon). The carbon present in the fused

oxide mixture activates the carbothermic reduction which may give lower oxides or respective metals as per equations 6.5-6.12 mentioned above. This molten slag layer is mainly responsible for the formation of the reduced metals which is alloyed by the iron bath. This slag may exist in three hypothetical layer. The top most layer of the slag is exposed towards the plasma arc zone which acts as a gas-slag interface, whereas, the bottom most layer of slag would act as a slag-metal interface. Due to the graphite crucible, the iron bath would be carbon saturated by absorbing carbon from the surface of the graphite crucible.

Case A: Consider a situation (Figure 6.13) when a charge is containing only mixture of bottom ash and carbon content. The silica and alumina of the charge material will be reduced by carbon to their respective lower oxides or metals. Aluminium monoxide and silicon monoxide formed as gaseous phase may try to move upward. These oxides may react with carbon present in the slag, to form their respective metals (Al and Si). If such reaction occurs in the slag-metal interfacial zone then the aluminium would be alloyed immediately by the liquid iron bath. In view of possibility of such reaction occurring in the intermediate layer of the slag, the produced aluminium metal vapor may move upwards. This aluminium vapor may also form aluminium-silicon alloy by combining with reduced silicon present in that zone. Due to the similar densities of silicon, aluminium-silicon alloy and slag may co-exist in this region. But due to high arc pressure, increased weight of gradually produced slag may push down the silicon, aluminium-silicon alloy towards the metal-slag interface followed by its alloying with the liquid iron bath. If such reaction takes place in the topmost layer (i.e. gas-slag interface), where very high-temperature zone exist, then all the reduction products may be present in the form of vapor. All these products would try to escape out. The presence of powder sample above the melt, may restricts its exit and push it back to the lower slag layer again.

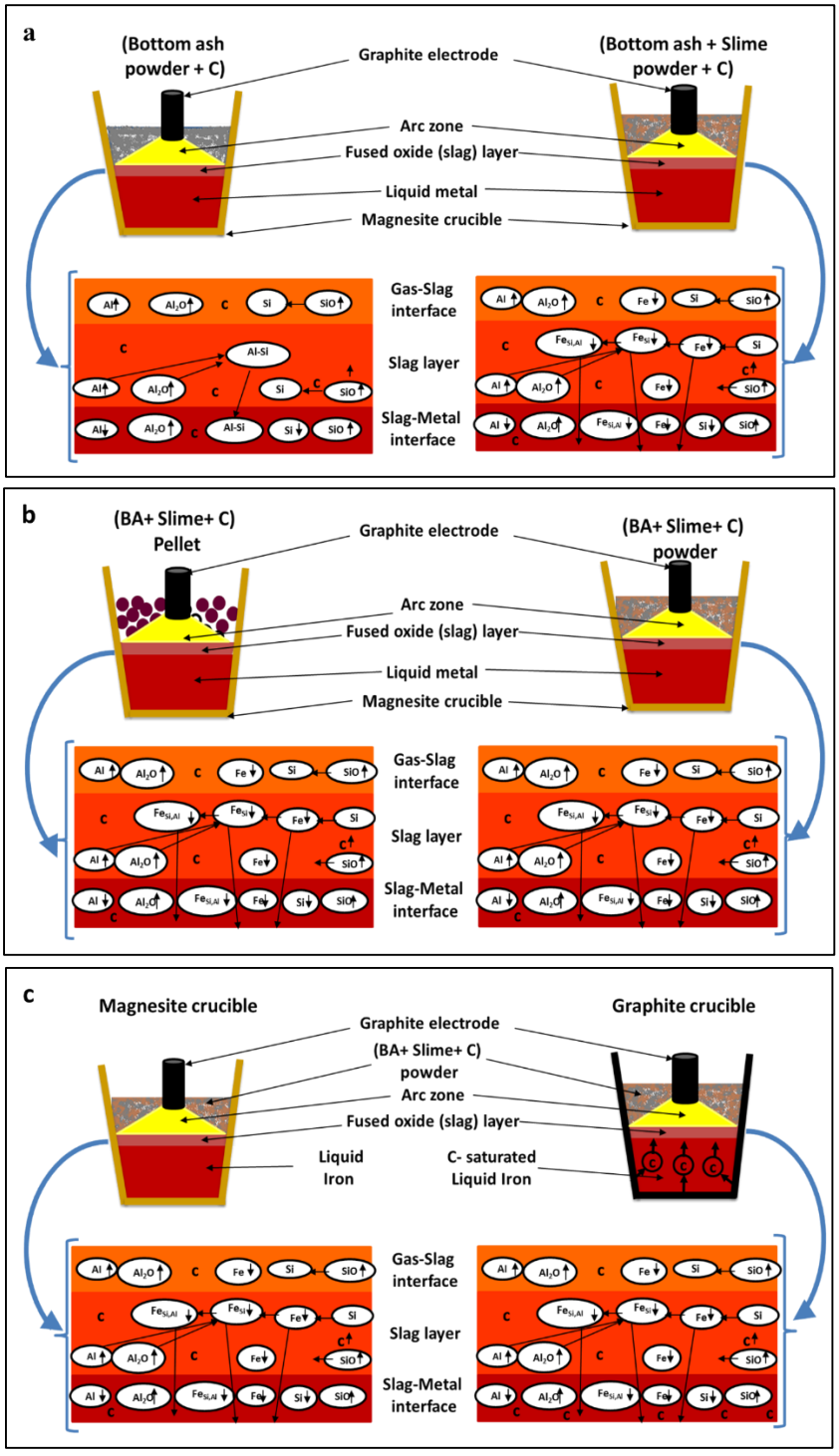

Figure 6. 13 Tentative mechanism of smelting reduction a) effect of charge chemistry, b) effect of charge forms, c) effect of lining material

Case B: In the case of charge in the form of pellets the increased inter-pellet voids, could give free passage to this metal vapor, resulting in lower recovery of metals (Al, and Si) which was observed experimentally.

In both cases (A & B), the charge containing the mixture of bottom ash, iron ore slime, and carbon, the iron oxide present in the mixture first gets reduced by carbon to liquid iron at that temperature to form an iron droplet in slag layer. Due to the higher density of liquid iron droplet, it easily moves downwards to meet liquid iron bath passing through the molten slag. During this downwards travel, iron drops alloy with reduced aluminium and silicon giving aluminium silicon alloy. This explains the higher aluminium metal recovery in case of charge containing iron ore slime and bottom ash as compared to only bottom ash. The manganese oxide if present may also get reduced at arc temperature and would form liquid manganese droplet which has higher density. The high density manganese droplets easily move down to alloy with iron in bath resulting in increased recovery.

Case C: When graphite crucible was used then crucible carbon dissolves in iron bath to saturate it with carbon. The carbon of the saturated iron bath causes reduction of the oxides present at the slag-metal interface into their respective metals followed by alloying with the iron bath instantly. This explains the higher recovery of the elements (Al and Si) while using graphite crucible as compared to magnesite crucible.

6.4 Conclusions

1. The present investigation indicates the feasibility of plasma arc smelting of iron ore slime and bottom ash to produce iron aluminium silicon alloy.

2. The partial recovery of aluminium and silicon in the steel bath is indicative of carbothermic reduction of alumina and silica in the charge at plasma arc temperature.

3. The recovery of aluminium and silicon due to carbothermic reduction under plasma arc appears to be affected by various operating parameters such as temperature, stoichiometric ratio of carbon in reductant, form of feeds (pellet/powder), charge material quantity, type of feed (bottom ash/ bottom ash + iron ore slime) and crucible lining.

In the present investigation, the limited experimentations have indicated the following trends:

1. Higher melt temperature by using hydrogen plasma appears to give more recovery of aluminium and silicon in the bath
2. The recovery of aluminium and silicon in the bath was found to increase with carbon content in the mix upto certain level (stoichiometry). Further addition did not affect the recovery.
3. The higher metal recovery (Al/Si) during smelting was noted while charging in powder form as compared to pellets.
4. Increased metal recovery was observed while charging large quantity of charge material (i.e. increased bed height/ charge layer thickness).
5. The higher metal recovery was observed in case of iron ore slime and bottom ash charge in comparison to bottom ash charging.
6. The higher metal recovery was also noted when graphite crucible was used as compared to magnesite crucible.